Heterogeneous & Homogeneous & Bio- & Nano-

CHEMCATCHEM

CATALYSIS

Accepted Article

Title: "Synthesis and Characterization of Ag@g-C3N4 and its photocatalytic evolution in visible light driven synthesis of ynone''

Authors: Dilip Virjibhai Vasava and Sunil Patel

To be cited as: *ChemCatChem* 10.1002/cctc.201901802

Link to VoR: http://dx.doi.org/10.1002/cctc.201901802

A Journal of ChemPubSoc Europe

WILEY-VCH

www.chemcatchem.org

“Synthesis and Characterization of Ag@g-C_3N_4 and its photocatalytic evolution in visible light driven synthesis of ynone’’

Sunil B. Patel[a] and Dilip V. Vasava*[b]

Abstract: The primary aim of this work is to synthesize photocatlyst to promote the synthesis of ynones. In this context, we synthesized AgNPs@g-C_3N_4 nanocomposite. The nanocomposite was characterized by using SEM, HR-TEM, XRD, EDS, ICP-AES, Uv-Vis DRS, XPS, PL and FT-IR. From the results of characterization, it was transpired that the AgNPs anchored firmly on the carbon nitride sheet and the size of nanoparticles ranges between 2-6 nm. We utilized the photoactive nanocomposite for the synthesis of various substituted ynones under visible light irradiation. Excellent yields were generated for the various substituted ynones (74-84 %). Furthermore, we study the gram scale synthesis and achieved yield up to 78 %. Recyclability of the nanocomposite was also studied and found that the material was recyclable up to 4 times without any significant loss in its activity. We have used 80 W tungsten bulb (λ > 420 nm) as the light source and GVL (gamma Valero lactone) as the solvent which proves the process much greener as compared to the conventional methods.

Introduction

The environmental issues are drastically increasing day by day and as a result, human facing major problems such as water, air, soil adulteration because of major chemical industries. Due to that, the natural resources affected rapidly and cause many serious issues. So, to overcome such problems research efforts have been made for cleaner and greener production by using photocatalysis.[1-9] Photocatalysis is one of the widely studied topics because of its wide range applicability. Many researchers have made the efforts to develop the sustainable catalytic approaches for the cleaner production. [10-15] Several photo catalytic protocols have been reported in the visible light irradiation to reduce the water contamination like waste water treatment [16], Dye degradation [17-21], degradation of organic pollutants [22-26] , H_2 production and CO_2 reduction [2-4] Furthermore, photocatalysis covers broad area of organic transformation such as, cross-coupling reaction,[27-29] trifluoromethylation [30-31] ,decarboxylative coupling reaction [32-37] , cycloaddition reaction [38] , deboronative alkynylation [39] , Aza- Hanry reaction [40] , dehalogenation reaction [41] , C-C and C-P bond formation reaction [42] , oxidation [43] , intermolecular addition reaction[44], Indole functionalization [45] , C-H functionalization [46] , heterocycle synthesis & functionalization [47] and etc.

Ynones (α, β-acetylenic ketone), have numbers of application in synthetic chemistry. They are involved in biologically active components and utilized as vital building blocks in heterocycle synthesis (Figure 1). The presence of carbonyl and the polarized alkyne group makes ynones more reactive intermediate.[48]

Ynones are important intermediates for the construction of heterocyclic compounds such as furan[49-50] , dihydropyranones [51] , pyroline[52] , pyrolle[53] , N- sulfinamines[54] , triazine[55] , spyrobaciline[56] , pyrazoles[57-60] , oxazepines, and oxazines[61] , diazepines[62] , triazoles[63] , quinolones[64] and annulation.[65] Various synthetic methods for the synthesis of ynones have been reported by using various metals like magnesium[66] , silver[67] , cadmium[68] , silicon[69] , copper[70] , tin[71] , lithium[72] , gallium[73] , stibium[74] , indium[75] , zinc[76] and boron.[77]

In the recent years, polymeric graphitic carbon nitride (g-C_3N_4) has gain more attention as a photocatalyst switching under visible light irradiation. Because of the lower band gap of 2.7 eV, this material has been extensively explored as an advanced modern semiconductor for the photocatalytic applications.[78] Taking inspiration from this, we synthesized Ag@g-C_3N_4 nanocomposites for the catalytic application. We applied synthesized nanocomposite for the catalytic evolution in cross-coupling reaction between benzoyl chloride and phenylacetylene in the presence of visible light irradiation (λ > 420 nm and intensity 11 candela).

---

[a] Mr. S. B. Patel
School of Sciences, Department of chemistry, Gujarat University
Navrangpura Ahmedabad-380009.
E-mail: skpatel111812@gmail.com

[b] Dr. D. V. Vasava
School of Sciences, Department of chemistry, Gujarat University
Navrangpura Ahmedabad-380009.
E-mail: dilipvasava20@gmail.com

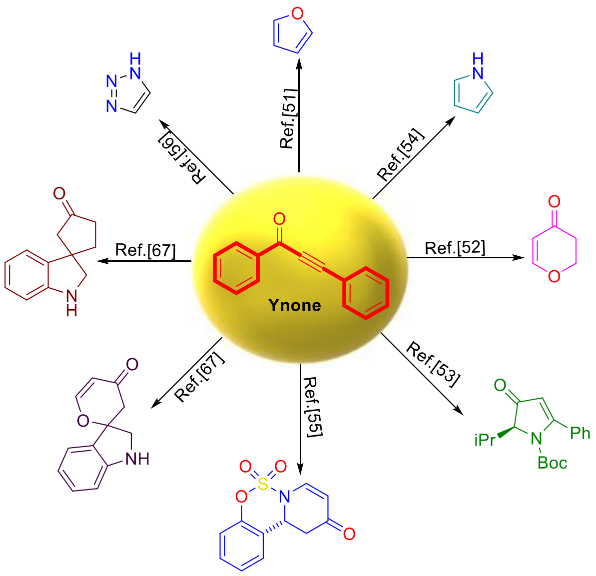

Figure 1. Application of ynone in construction of various heterocycles and annulation.

Results and Discussion

Photocatalysis is an important area of research in catalysis. The g-C_3N_4 was having many properties of heterogeneous catalyst as well as photocatalyst. Furthermore, it has high surface area, stability and photo catalytic activity, and it has proved a very interesting supporting material for photocatalysis. As a part of our study we synthesized and characterized the catalyst by using SEM, HR-TEM, EDX, XRD, Uv-Vis DRS, XPS, PL, FT-IR and ICP-AES.

The morphology of synthesized samples was investigated though SEM analysis. the SEM images of synthesized g-C_3N_4 and AgNPs@g-C_3N_4 nanocomposite were given. The pure carbon nitride reflects an aggregated particle which were larger in size. On later investigation we observed the morphology of carbon nitride was like flower petal. The layered surface of the aggregation is smooth. After the encapsulation of silver nanoparticles, the morphology did not affect but the surface was seemed to be rough. Both the figures were given below which (Figure 2a) indicates surface of carbon nitride before encapsulation and (Figure 2b) after encapsulation of AgNPs.

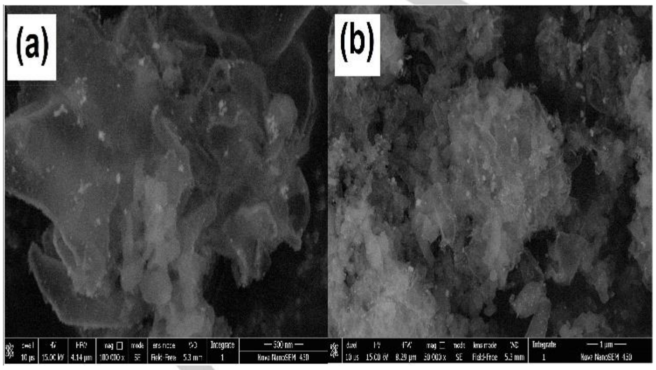

Figure 2. SEM image (a) g-C_3N_4 (a) and (b) AgNPs@g-C_3N_4.

To evaluate the phase and crystal structure of the synthesized nanocomposites, the prepared samples were analyzed by XRD. In figure 3 the XRD pattern of g-C_3N_4 and AgNPs@g-C_3N_4 was given. In the XRD pattern of g-C_3N_4 one broad peak at 27.4° 2θ was observed and it was associated with (0 0 2) plane with d = 0.322 nm. The high and intense peak at 27.4° 2θ was attributed to the high interplanar stacking of the aryl re-arrangement which referred as the (0 0 2) plane of g-C_3N_4 (ICCD card no 87-1526) (Figure 3a). In Ag@g-C_3N_4 nanocomposite sample XRD shows five different reflections including one peak of g-C_3N_4. The X-Ray Diffraction peaks at 38.4°, 44.0°, 64.4° and 77.42° were referred to (1 1 1), (2 0 0), (2 2 0) and (3 1 1) planes for silver nanoparticles (Figure 3b). The observed pattern and reflection planes are in good agreement with the standard pattern of AgNPs (ICCD card no. 04-0783).[79] The peak intensity intended the low loading of Ag^+ ions on graphitic carbon nitride. In the second spectrum the extra peaks except g-C_3N_4 confirmed the encapsulation of AgNPs on g-C_3N_4. The average crystallite size of the AgNPs was calculated by using Scherer's formula. From the above discussed results, we can say the AgNPs having face cantered cubic (fcc) symmetry and having crystalline nature.

$$D = \frac{K\lambda}{\beta \text{ Cos } \theta}$$

10.1002/cctc.201901802

Where D = average grain size; K = shape factor with a value of ~0.9; λ = x-ray wavelength (Cu Kα = 0.15405 nm); β = (FWHM) full width at half-maximum (in radians); and θ = Bragg's angle. The calculated average grain size of AgNPS@g-C_3N_4 were 4-8 nm.

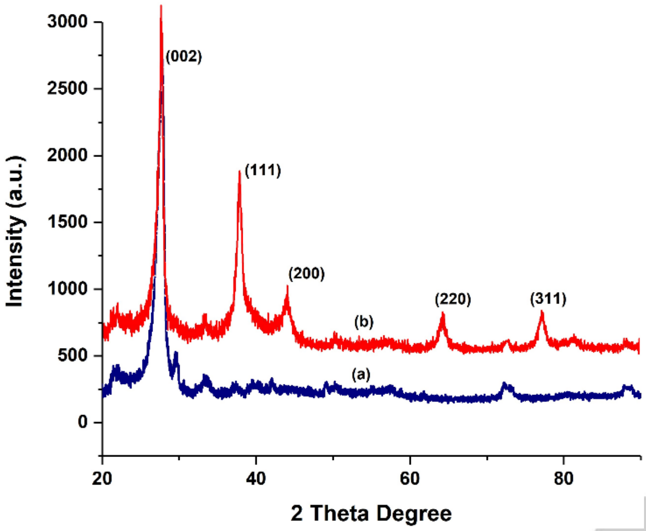

Figure 3. X-ray diffraction pattern of g-C_3N_4 (a) and AgNPs@g-C_3N_4 (b).

To find out more information regarding the morphology, particle size and shape of prepared sample AgNPs@g-C_3N_4 was examined through TEM and HR-TEM analysis. As shown in (Figure 4), the black coloured spots were referred to silver nanoparticles and grey coloured area ascribed to surface of g-C_3N_4. The synthesized material is capable to absorb visible light. The grey surface in TEM image of g-C_3N_4 is capable to absorb visible light. In figure it's clearly seen that the interfacial contact of silver nanoparticles with g-C_3N_4 sheet, which enclosed the whole surface area of the sheet. From the figure we can concluded the encapsulated AgNPs were spherical in shape and size as measured between 2-6 nm. Furthermore, no agglomeration of AgNPs were observed which is very good thing from the aspects of heterogeneous catalysis. SAED pattern of nanocomposites showed bright rings, specifying that the nanocomposite is highly crystalline in nature. The bright fringes appeared were attributed to (1 1 1), (2 0 0), (2 2 0) and (3 1 1) planes for metallic silver species.

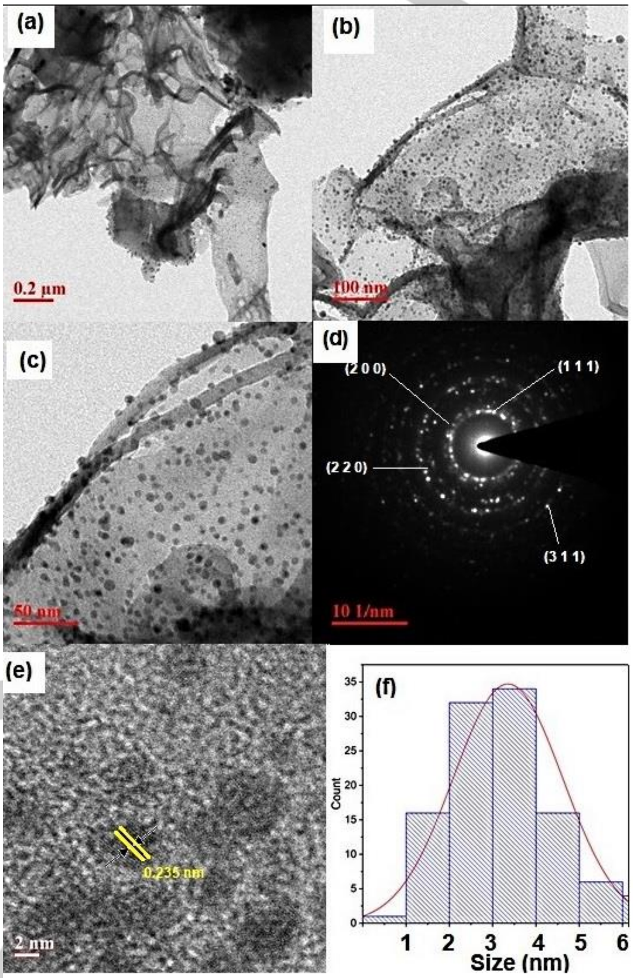

Figure 4. TEM images of AgNPs@g-C_3N_4 (a) at 0.2 um scale (b) at 100 nm scale (c) at 50 nm scale (d) SAED pattern (e) HR-TEM image of AgNPs (f) Particle size distribution curve.

For elemental information of the silver nanocomposites EDX mapping of selected area was carried out. In (Figure 5) the peak appeared near 0.3 and 3.0 keV confirmed the presence of silver species in nanocomposites. In the mapping image different colour appeared and they were attributed to different elements which was further clarified in images where red colour was for silver. The red coloured dots were very less in the image hence we concluded that the loading of metal was very low in synthesized nanocomposite. Furthermore, loading of silver was found 0.0531 mmol/gm from ICP-AES analysis.

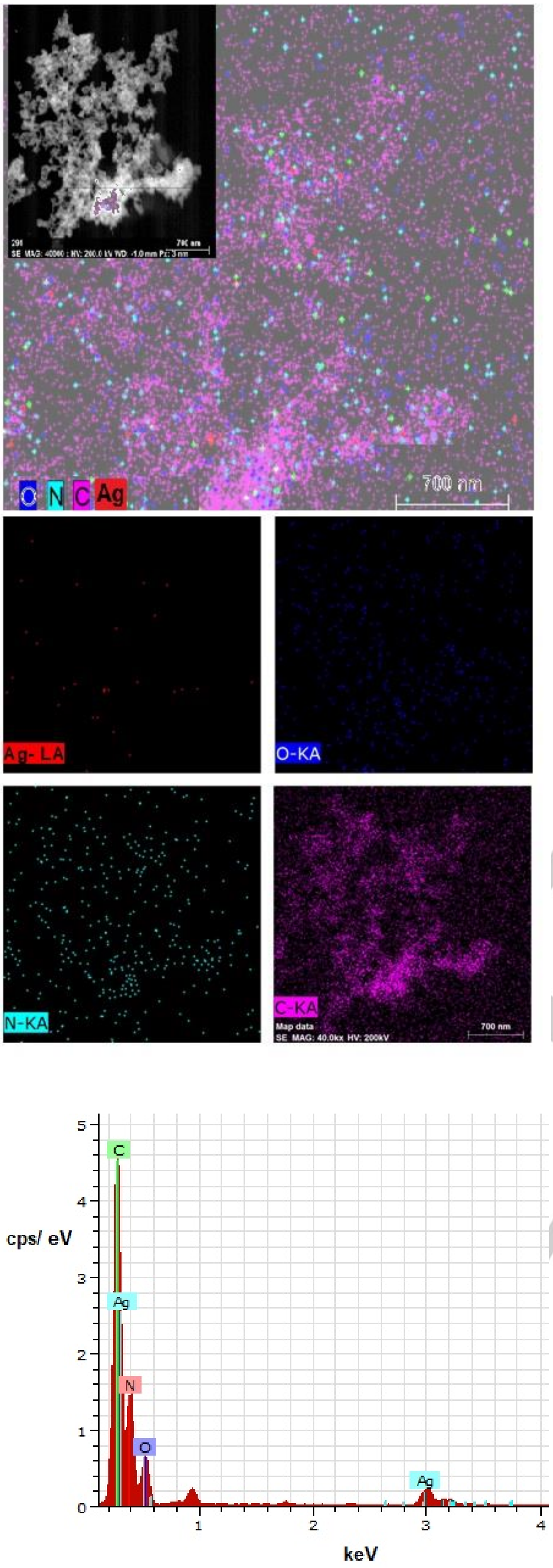

Figure 5. EDX mapping image of AgNPs@g-C_3N_4.

Typical FT-IR spectrum of silver nanocomposites was shown in (Figure 6). As the material consist of triazine units the breathing of triazine units can be seen at 796-808 cm^{-1}. Here peaks appeared at 1171 cm^{-1}, 1438 cm^{-1} and 1671 cm^{-1} indicated the C-N stretching of heterocycle and revelling the information about C-N-C linkages[79] present in the material. Here we can see there was no significant changes in the fresh nanocomposite and nanocomposite after fourth cycle.

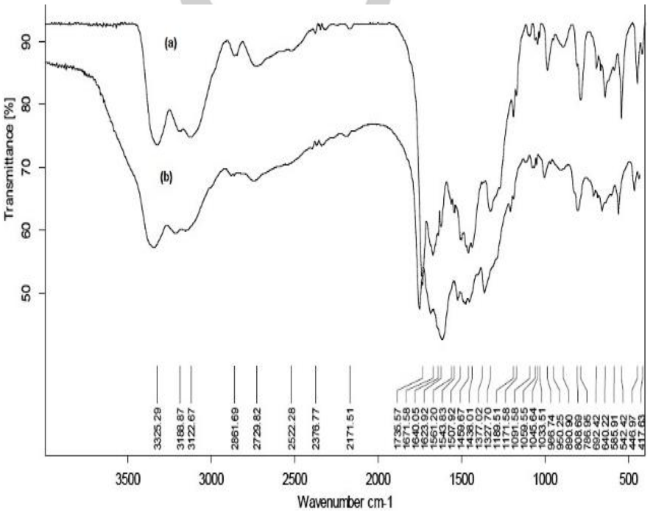

Figure 6. FT-IR images of (a) Fresh AgNPs@g-C_3N_4 and (b) Recycled AgNPs@g-C_3N_4.

For the deeper investigation of elemental composition and oxidation state of AgNPs@g-C_3N_4 XPS was carried out (Figure 7). The four elements (C, N, O, Ag) could be seen in the survey spectrum of AgNPs@g-C_3N_4. The peak arise at 287.67 eV and 292.59 eV were denoted as C 1S peaks, which also revealing the information about the sp^2 hybridized carbon atoms and N-C-N bonding in the g-C_3N_4. The peak arise at 399.18 eV was denoted as N 1S peak, which significantly indicating the presence of sp^3 hybridized N atoms and C-N-C linkages in the synthesized material. [80,81] In the spectrum of Ag 3d the peaks arise at 367.18 eV and 373.16 eV can be denoted as Ag $3d_{5/2}$ and Ag $3d_{3/2}$. The XPS results confirmed that the Ag nanoparticles firmly anchored on the surface of g-C_3N_4.

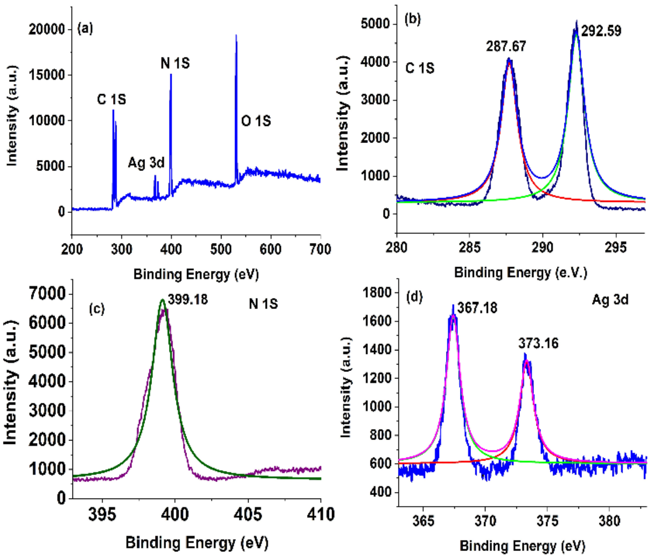

Figure 7. XPS spectra of Ag@g-C_3N_4 (a) XPS servey spectrum (b) High resolution spectrum of C 1S (c) High resolution spectrum of N 1S (d) High resolution spectrum of Ag 3d.

UV-Vis Diffuse Reflectance Spectra

To study the optical absorption ability of the synthesized samples, the UV–vis DRS analysis was carried out. The spectral measurements of pure g-C_3N_4 and Ag@g-C_3N_4 was carried out. As shown in (Figure 8), the pure g-C_3N_4 existed good absorption performance in the visible light region. The absorption edge of the synthesized sample was estimated at about 450 nm, and the band gap value was determined to be 2.72 eV for g-C_3N_4. For the Ag@g-C_3N_4, the absorption capability was notably enhanced as compared to the g-C_3N_4. In the spectra it was clearly seen that the distinct red shift took place around 450-600 nm, which was took place due to the SPR (silver surface plasmon resonance). The results could elaborate that the optical absorption ability was increased due to the Ag species. It was notable that the absorption spectra of Ag@g-C_3N_4 are better than g-C_3N_4. The enhanced optical absorption capability will upsurge the photocatalytic activity. The UV-DRS measurement results proved that the Ag played a crucial role to intensify the photocatalytic activity of Ag@g-C_3N_4.[81]

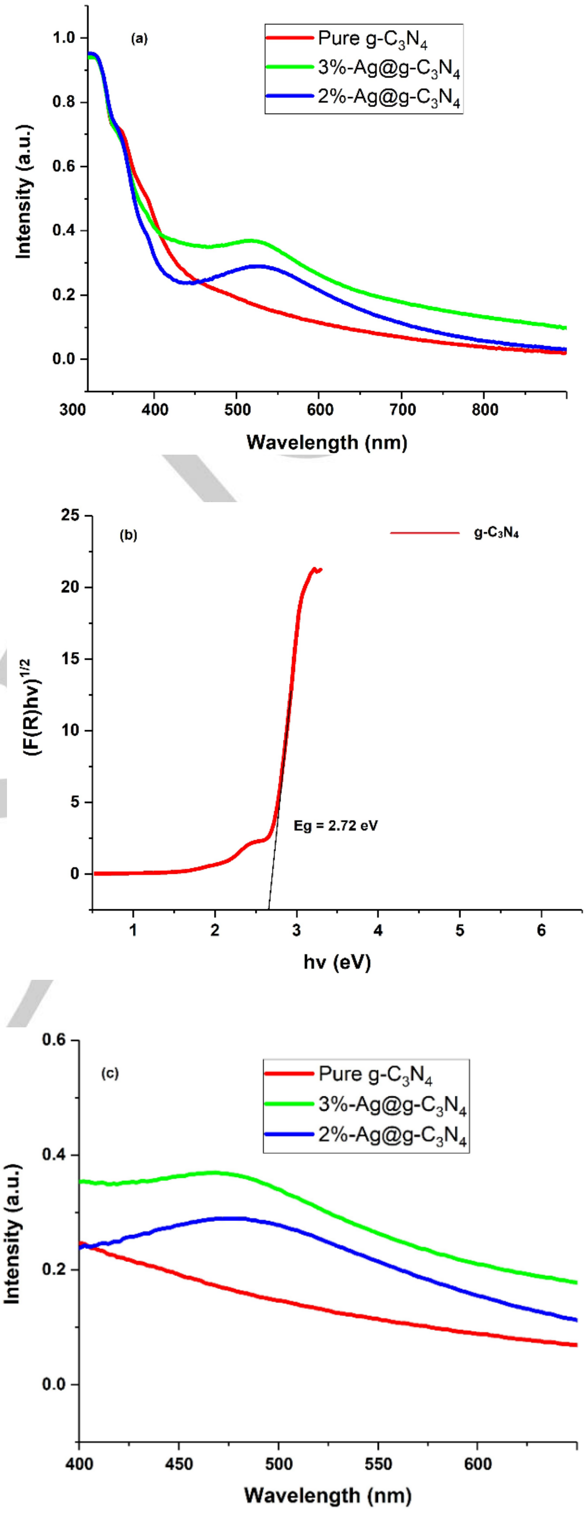

Figure 8. (a) UV-Vis DRS spectra of g-C_3N_4 and 2% Ag@g-C_3N_4 , 3% Ag@g-C_3N_4 (b) Band gap determination of g-C_3N_4 (c) SPR cherecteristics of Ag.

To measure the separation capability and life time of photogenerated carrier's photoluminescence (PL) measurement was used. Photoluminescence spectra of g-C_3N_4 and Ag@g-C_3N_4 were shown in figure 9. the excitation wavelength used is 325 nm during the experiment. A strong peak was observed near 450 nm, from the comparison of both the spectra, we observed the photoluminescence intensity of g-C_3N_4 is relatively more than the Ag@g-C_3N_4. The weaker peak intensity showed a slower recombination rate of photogenerated carriers. On the other hand, the presence of Ag NPs present at the surface of g-C_3N_4 effectively slower down the recombination rate of electrons and hole pairs. This leads the e^- and h^+ to facilitates the photo catalytic process of Ag@g-C_3N_4.[81]

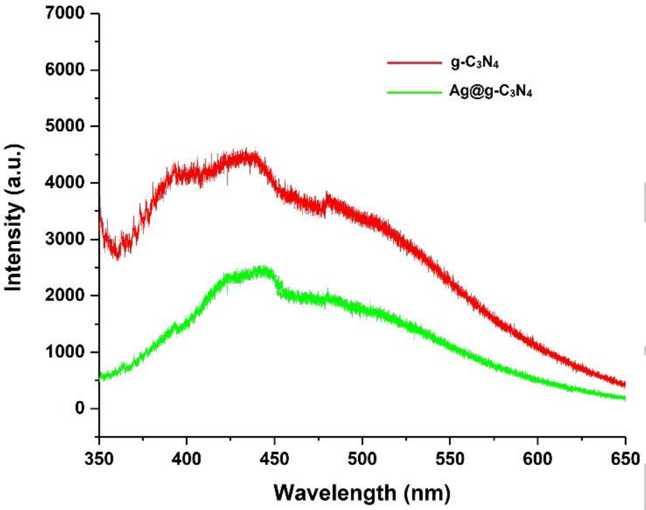

Figure 9. PL spectra of pure g-C_3N_4 and Ag@g-C_3N_4.

Light driven catalytic evolution of AgNPs@g-C_3N_4 for the synthesis of ynone

After successfully characterizing the nanocomposite, we planned to examine its catalytic efficacy in the cross-coupling reaction between benzoyl chloride and terminal alkynes. As we discussed earlier, our aim was to develop efficient and greener conditions for the synthesis of ynones. We mainly focused on greener reagents and reusability of material. For this, we chose the reaction between benzoyl chloride and phenyl acetylene as the model substrates. A 80 W tungsten filament blub was used as the irradiation source (λ > 420 nm) scheme 1.

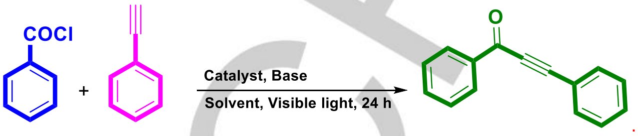

Scheme 1. Synthesis of ynone from benzoyl chloride and phenylacetylene.

Table 1. Screening of cross-coupling reaction between benzoyl chloride and phenylacetylene under different conditions

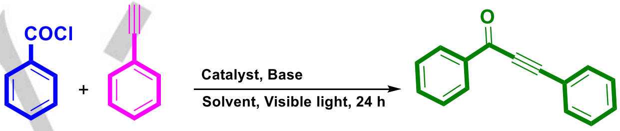

Entry	Catalyst	Solvent	Base	Yield [b]
1	Ag@g-C_3N_4	Ethylene glycol	Et_3N	52 %
2	Ag@g-C_3N_4	PEG-100	Et_3N	50 %
3	Ag@g-C_3N_4	PEG-200	Et_3N	40 %
4	Ag@g-C_3N_4	GVL	Et_3N	84 %
5	Ag@g-C_3N_4	Propylene carbonate	Et_3N	75 %
6	Au@g-C_3N_4	GVL	Et_3N	64 %
7	Cu@g-C_3N_4	GVL	Et_3N	69 %
8	Pd@g-C_3N_4	GVL	Et_3N	65 %
9	Ag@g-C_3N_4	GVL	K_2CO_3	10 %
10	Ag@g-C_3N_4	GVL	Na_2CO_3	14 %
11	Ag@g-C_3N_4	GVL	Cs_2CO_3	12 %
12 [c]	Ag@g-C_3N_4	GVL	Et_3N	No reaction

[a] Reaction conditions: Benzoyl chloride (1.1 mmol), phenylacetylene (1.2mmol), Base (2 mmol), Catalyst (100 mg), Solvent (2 mL), under N_2 atm., 80 W tungsten blub, 24 h. GVL = gamma Valero lactone.

[b] Isolated yields, [c] in dark conditions.

10.1002/cctc.201901802

Here we were selected only greener solvents which were available easily and unharmful for the environment. As a prospectus to obtain benign conditions we scan the experiment in ethylene glycol (EG), PEG-100, PEG-200, gamma Valero lactone (GVL) and propylene carbonate. After scanning the solvents, we found good results were obtained in gamma Valero lactone and achieved yield up to 84 % table 1 (entry 1 to 5). Some other nanocomposites were used such as Au@g-C_3N_4, Cu@g-C_3N_4 and Pd@g-C_3N_4 table 1 (entry 6, 7, 8) but best results were obtained with the Ag@g-C_3N_4. Bases such as Et_3N, K_2CO_3, Na_2CO_3 and Cs_2CO_3 table 1 (entry 4, 9, 10, 11) were incorporated in the reaction. Amongst them results obtained with Et_3N were optimum. In rest of the inorganic bases desired product was not obtained in good yield the results have been mentioned in table 1. Furthermore, the reaction carried out in absence of base, but the reaction was not initiated. Hence, we concluded that the basic medium was required to carry out the reaction. Similar results were obtained while the reaction was carried out in absence of nanocomposite and in absence of light.

Hence by taking the optimized reaction conditions further reactions were carried out. The scope of the reaction was further generalized by using different substituted benzoyl chlorides and terminal acetylenes. Better group tolerance was observed under optimized photocatalytic conditions. We have used bicyclic benzoyl chloride, -methoxy, -methyl and -chloro substituted benzoyl chlorides all the substituted derivatives provided excellent yield up to 70-84 % [table 2 (entry 1 to 8)]. Correspondingly, in substituted alkynes such as -Cl, -Br, -F, $-CH_3$, $-OCH_3$ we were obtained excellent yield up to 80-84 % [table 2 (entry 9 to 13)]. However, in aliphatic alkynes the expected yield was lower in the case of cyclopropyl acetylene 76 % yield was obtained and in 1-hexyne yield was declined to 74 % [table 2 (entry 14, 15)]. Conclusion drawn from the obtained results that the aromatic substituted benzoyl chloride and acetylene reacted well to give corresponding ynones in excellent yield.

[a] Table 2. AgNPs@g-C_3N_4 catalyzed cross coupling reaction between Substituted benzoyl chloride and terminal alkynes

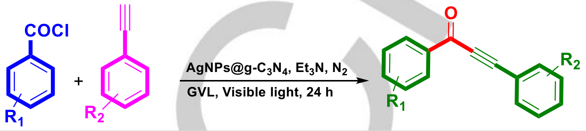

Entry	Reactant	Product	% Yield [b]
1	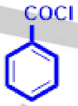	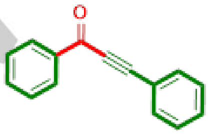	84
2	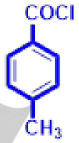	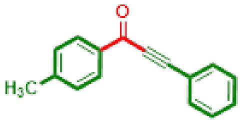	81
3	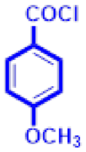	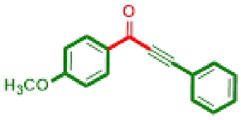	80
4	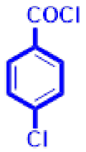	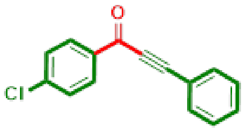	84
5	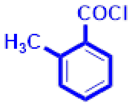	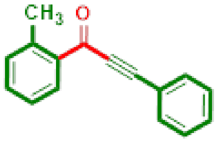	82
6	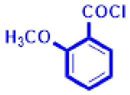	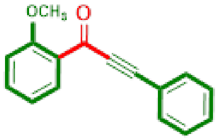	82

10.1002/cctc.201901802

7	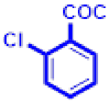	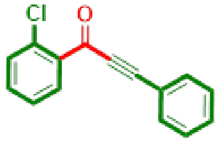	80
8	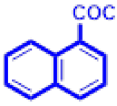	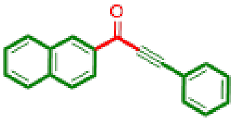	79
9	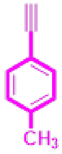	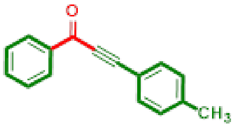	84
10	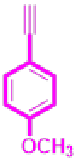	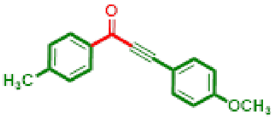	83
11	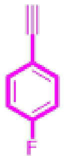	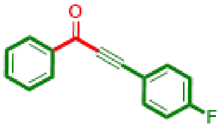	84
12	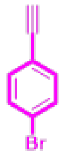	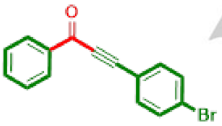	80
13	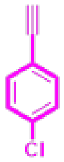	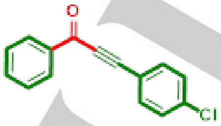	80
14	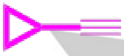	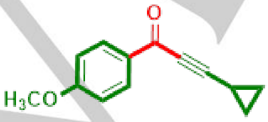	76
15		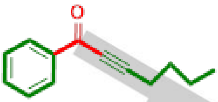	74

[a]Reaction conditions: Benzoyl chloride (1.1 mmol), phenylacetylene (1.2mmol), Et_3N (2 mmol), Catalyst (100 mg), GVL (2 mL), under N_2 atm., 80 W tungsten blub, 24 h. GVL = gamma Valero lactone.[b] Isolated yields.

Gram scale synthesis of ynone

Scale up synthesis is one of the important factors in heterogeneous catalysis. We scanned synthesized nanomaterial for the scale up synthesis by taking 5.0 gm of the initial reactant. The reaction was stirred under visible light irradiation for 24 h under optimized reaction condition and 3.90 gm of ynone (78% yield) was obtained.

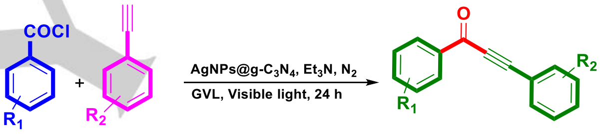

Scheme 2. Gram scale synthesis of ynone.

Photocatalytic Mechanism

The probable photocatalytic mechanism for the synthesis of ynone is discussed based on SPR effect of Ag species and decreased rate of the recombination of photogenerated e^- and h^+ pairs. Modification of g-C_3N_4 with silver nanoparticles increased the photocatalytic performance of Ag@g-C_3N_4. When Ag@g-C_3N_4 irradiated to visible light source (80 W tungsten bulb, λ > 420 nm), the e^- and h^+ pairs are separated, e^- is excited and moved to CB of g-C_3N_4 while on the other hand, h^+ stay at VB of g-C_3N_4. Then e^- transfers to Ag nanoparticles due to the high Schottky barrier.[81] Finally, transfer takes place to the surface of photocatalyst to join the formation of silver acetylide complex with terminal acetylene in presence of base and reaction facilitates towards the formation of ynone.

Recyclability Study

Recyclability is an important factor which affects the performance of the heterogeneous nanomaterial. So, we carried out the recyclability studies of the synthesized nanocomposite. In that context, the recovered catalyst obtained after first cycle were washed thrice with absolute alcohol and dried prior to reuse. We repeated the same procedure for 4 times, after the fourth cycle, the activity of nanocomposite gradually reduces. So, we conclude that we can use the nanocomposite at least 4 times without any significant loss in its catalytic activity (Figure 10). Furhtermore, we investigate the resone behind the reduced activity after fourth cycle. We found that the loss of catalyst during the recovery process may be responsible for the decreasing activity of the catalyst.

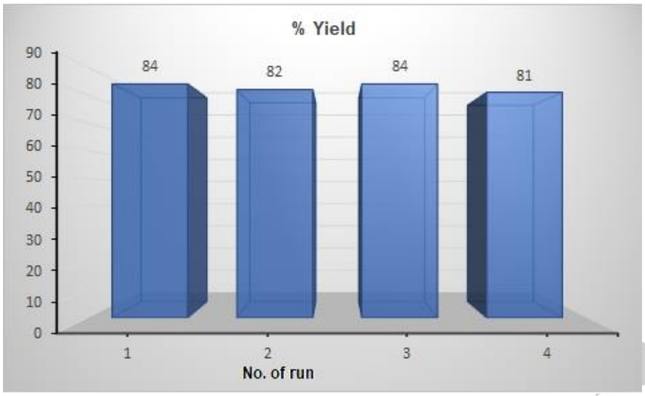

Figure 10. Recyclability image of AgNPs@g-C_3N_4.

Post recyclability studies were also carried out to ensure the stability of the catalyst. TEM, XRD and XPS analysis were carried out to ensure the stability of catalyst under optimized reaction conditions. TEM, XRD and XPS analysis were given in (Figure 11), from the results we can concluded that there was no notable changes observed in the catalyst after the reaction.

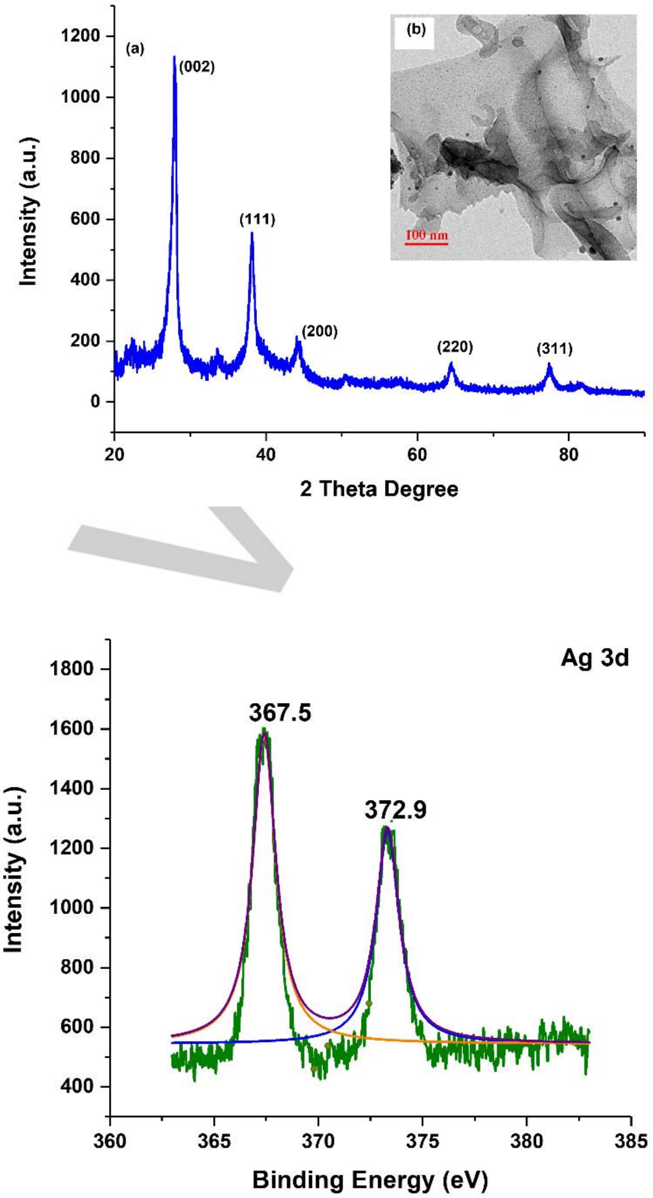

Figure 11. Post reaction XRD, TEM and XPS of AgNPs@g-C_3N_4.

Conclusions

In conclusion, AgNPs@g-C_3N_4 has been developed and characterized by sophisticated techniques such as, SEM, HR-TEM, EDX, XRD, ICP-AES, XPS, Uv-Vis DRS, PL and FT-IR. In TEM and HR-TEM analysis results we found the size of the AgNPs were in nano dimension (2-6 nm) and were highly crystalline in nature. Similar evidences were found in XRD analysis. Loading of metal was found very low (0.0531 mmol/gm) from ICP-AES analysis. After successfully characterization of nanocomposite, we have explored the photocatalytic activity of

$AgNPs@g\text{-}C_3N_4$. We have developed greener pathway for the access of various substituted ynones under visible light irradiation (λ > 420 nm). Furthermore, we have utilized only greener solvents which were environmentally friendly.

Experimental Section

Materials

All chemicals were used of analytical grade and of the highest purity available. Benzoyl chloride, and terminal acetylenes were purchased from Sigma-Aldrich. Ethyl acetate, ethanol, hexane and $NaBH_4$ were purchased from TCI. Water used in all experiments was purified by Millipore-Q system. All glassware was thoroughly washed with aqua regia.

Synthesis of carbon nitride ($g\text{-}C_3N_4$)

Synthesis of carbon nitride was done according to the literature. [80]

Preparation of $Ag@g\text{-}C_3N_4$ nanocomposite

$Ag@g\text{-}C_3N_4$ nanocomposite was synthesized by a sorption reduction method. Firstly, prepared solution of 1.0 mmol $AgSO_4$ in deionized water with 2 gm of carbon nitride powder was added in the solution with continuous stirring. After 1 h the Ag^+ ions were reduced by passing cold $NaBH_4$ solution at 10 °C. Excess of reagents were removed by washing with deionized water and finally washed with ethanol. Resultant nanocomposite was dried in oven at 60 °C for 10 h.

General procedure for the synthesis of ynone

Take 1.1 mmol of benzoyl chloride and 1.2 mmol of Phenylacetylene in10 mL RBF add 100 mg of $Ag@g\text{-}C_3N_4$ nanocomposite and 2 mL solvent. Stirred the reaction mixture at room temperature and add appropriate amount of Et_3N (2 mmol), further the reaction mixture was purged with N_2 and put the reaction mixture under visible light irradiation source (80 W tungsten bulb, λ > 420 nm) with continuous stirring. Check the progress of reaction by TLC (hexane/ethyl acetate 9:1), after 24 h the reaction was completed. After completion of the reaction, quenched the reaction mixture in ice water and extracted with ether. Wash the ether layer with brine solution and dried over anhydrous $MgSO_4$. The solvent was removed under reduce pressure to get the desired crude product. The crude product was further purified by column chromatography (hexane/ethyl acetate 100:1), and analyzed by ^1H NMR and ^{13}C NMR.

Acknowledgements

The authors are grateful to, MNIT, Jaipur for SEM, HR-TEM, XRD, XPS, PL and EDX analysis, SAIF, Punjab University, Chandigarh, for the ^1H-NMR and ^{13}C-NMR analysis. Authors are also grateful to, Department of physics, school of sciences, gujarat university for Uv-Vis DRS analysis specially Dr. U. S. Joshi and his research students Poornima Sengunthar, Nisha Thangachen and Shivangi patel.

Conflict of interest

The authors declared no conflict of interest.

Keywords: Green approach • Heterogeneous catalysis • Silver nanocomposite • Visible light • ynone

10.1002/cctc.201901802

[1] X. Lang, X. Chen, J. Zhao, *Chem. Soc. Rev.* **2014***, 43*, 473-486.

[2] Y. Huo, J. Zhang, K. Dai, Q. Li, J. Lv, G. Zhu, C. Liang, *App. Catal. B: Env*. **2019**, *241*, 528-538.

[3] T. Hu, Z. Li, L. Lu, K. Dai, J. Zhang, R. Li, C. Liang, *J. Coll. Int. Sci.* **2019**, 555, 166-173.

[4] T. Hu, K. Dai, J. Zhang, G. Zhu, C. Liang, *Appl. Surf. Sci.* **2019**, *481,* 1385-1393.

[5] F. Mei, J. Zhang, K. Dai, G. Zhu, C. Liang, *Dalton Trans.* **2019**, *48,* 1067-1074

[6] Y. Huo, Y. Yang, K. Dai, J. Zhang, *Appl. Surf. Sci.* **2019**, *481*, 1260-1269.

[7] N. Zhang, Y. Zhang, M. Q. Yang, Y. J. Xu, *Curr. Org. Chem.* **2013,** *17,* 2503-2515.

[8] M. Q. Yang, Y. J. Xu, *Phys. Chem. Chem. Phys.* **2013**, 1*5*, 19102-19118.

[9] C. Han, Z. R. Tang, J. Liu, S. Jin, Y. J. Xu, *Chem. Sci*. **2019,** *10, 3514-*3522.

[10] C. Han, S. H. Li, Z. R. Tang, Y. J. Xu, *Chem. Sci.* **2018**, *9*, 8914-8922.

[11] Y. Zhang, N. Zhang, Z. R. Tang, Y. J. Xu, *Chem. Sci.* **2012**, *3,* 2812-2822.

[12] N. Zhang, M. Q. Yang, S. Liu, Y. Sun, Y. J. Xu, *Chem. Rev.* **2015,** *115,* 10307-10377.

[13] F. Mei, K. Dai, J. Zhang, W. Li, C. Liang, *Appl. Surf. Sci. 2019, 488,* 151-160.

[14] Z. Li, X. Wang, J. Zhang, C. Liang, L. Lu, K. Dai, *Chin. J. Catal. 2019, 40*, 326-334.

[15] Y. Huo, Z. Wang, J. Zhang, C. Liang, K. Dai, *Appl. Surf. Sci.* 2018, *459*, 271-280.

[16] S. Dong, J. Feng, M. Fan, Y. Pi, L. Hu, X. Han, J. Sun, *RSC. Adv.* **2015**, *5,* 14610-14630.

[17] M. Yin, Z. Li, J. Kou, Z. Zou, *Env. Sci. & tech.* **2009**, *43*, 8361-8366.

[18] S. W. Cao, Z. Yin, J. Barber, F. Y. Boey, S. C. J. Loo, C. Xue, *ACS app.mater. & inter*. **2011**, *4*, 418-423.

[19] P. Wang. B. Huang, X. Qin, X. Zhang, Y. Dai, J. Wei, M. H. Whangbo. *Angew. Chem. Int. Ed.* **2008**, *47*, 7931-7933.

[20] A. K. L. Sajjad, S. Shamaila, B. Tian, F. Chen, J. Zhang. *J. Hazardous Mat.* **2010**, *177*, 781-791.

[21] A. T. Kuvarega, R. W. Krause, B. B. Mamba. *J. Phy. Chem. C*. **2011**, *115*, 22110-22120.

[22] J. Tang, Z. Zou, J. Ye. *Angew. Chem. Int. Ed.* **2004**, *43*, 4463-4466.

[23] R. Abe, H. Takami, N. Murakami, B. Ohtani. *J. Am. Chem. Soci.* **2008**, *130*, 7780-7781.

[24] D. Chatterjee, S. Dasgupta. *J. Photochem. and Photobio. C:* **2005**, *6*, 186-205.

[25] D. Lu, H. Wang, X. Zhao, K. K. Kondamareddy, J. Ding, C. Li, P. Fang, *ACS Sus. Chem. & Eng.* **2017**, *5*, 1436-1445.

[26] C. Yu, G. Li, S. Kumar, K. Yang, R. Jin. *Adv. Mater*. **2014**, *26*, 892-898.

[27] S. Kim, J. Rojas-Martin, F. D. Toste, *Chemical science* **2016**, *7*, 85-88.

[28] S. Protti, M. Fagnoni, A. Albini. *Angew. Chem. Int. Ed.* **2005**, *44*, 5675-5678.

[29] M. De Carolis, S. Protti, M. Fagnoni, A. Albini, *Angew. Chem. Int. Ed.* **2005**, *44*, 1232-1236.

[30] W. Fu, W. Guo, G. Zou, C. Xu, *J. Fluorine Chem.* **2012**, *140*, 88-94.

[31] Y. Ye, M. S. Sanford, *J. Am. Chem. Soc.* **2012,** *134*, 9034-9037.

[32] F. Le Vaillant, T. Courant, J. Waser, *Angew. Chem. Int. Ed.* **2015**, *54*, 11200-11204.

[33] C. Yang, J. D. Yang, Y. H. Li, X. Li, J. P. Cheng, *J. Org. Chem.* **2016,** *81*, 12357-12363.

[34] J. Yang, J. Zhang, L. Qi, C. Hu, Y. Chen, *Chem. Commun.* **2015**, *51*, 5275-5278.

[35] T. Qin, L. R. Malins, J. T. Edwards, R. R. Merchant, A. J. Novak, J. Z. Zhong, P. S. Baran, *Angew. Chem. Int. Ed.* **2017**, *56*, 260-265.

[36] Q. Q. Zhou, W. Guo, W. Ding, X. Wu, X. Chen, L. Q. Lu, W. J. Xiao, *Angew. Chem. Int. Ed.* **2015**, *54*, 11196-11199.

[37] J. Liu, Q. Liu, H. Yi, C. Qin, R. Bai, X. Qi, A. Lei, *Angew. Chem. Int. Ed.* **2014**, *53*, 502-506.

[38] Z. Lu, M. Shen, T. P. Yoon, *J. Am. Chem. Soc.* **2011**, *133*, 1162-1164.

[39] H. Huang, G. Zhang, L. Gong, S. Zhang, Y. Chen, *J. Am. Chem. Soc.* **2014**, *136*, 2280-2283.

[40] A. G. Condie., J. C. González-Gómez., C. R. Stephenson. *J. Am. Chem. Soc.* **2010**, *132*, 1464-1465.

[41] T. Maji, A. Karmakar, O. Reiser, *J. Org. Chem.* **2010**, *76*, 736-739.

[42] D. P. Hari, B. König, *Org. Lett.* **2011**, *13*, 3852-3855.

[43] M. Rueping, R. M. Koenigs, K. Poscharny, D. C. Fabry, D. Leonori, C. Vila, *Chem.–A Eur. J.* **2012,** *18*, 5170-5174.

[44] R. S. Andrews, J. J. Becker, M. R. Gagné, *Angew. Chem. Int. Ed.* **2010**, *49*, 7274-7276.

[45] A. A. Festa, L. G. Voskressensky, E. V. Van der Eycken, *Chemical Society Reviews*. 2019. Visible light-mediated chemistry of indoles and related heterocycles. DOI: 10.1039/c8cs00790j

[46] M. Uygur, O. G. Mancheño, *Org. & Bio. Chem.* **2019**, *17*, 5475-5489.

[47] J. R. Chen, X. Q. Hu, L. Q. Lu, W. J. Xiao, *Acc. Chem. Res.* **2016,** *49*, 1911-1923.

[48] R. E. Whittaker, A. Dermenci, G. Dong, *Synthesis***, 2016**, *48*, 161-183.

[49] H. Sheng, S. Lin, Y. Huang, *Tetrahedron Lett.* **1986**, *27*, 4893-4894.

[50] A. V. Kel'i, V. Gevorgyan, *J. Org. Chem.* **2002**, *67*, 95-98.

[51] S. L. Shi, M. Kanai, M. Shibasaki, *Angew. Chem. Int. Ed.* **2012**, *51*, 3932-3935.

[52] N. Gouault, M. Le Roch, C. Cornee, M. David, P. Uriac, *J. Org. Chem.* **2009**, *74*, 5614-5617.

[53] Z. Wang, Y. Shi, X. Luo, D. M. Han, W. P. Deng, *N. J. Chem.* **2013**, *37*, 1742-1745.

[54] Y. Liu, T. R. Kang, Q. Z. Liu, L. M. Chen, Y. C. Wang, J. Liu, Y. M. Xie, J. L. Yang, L. He, *Org. Lett.* **2013**, *15*, 6090-6093.

[55] S. Hwang., H. Bae., S. Kim., S. Kim. *Tetrahedron*, **2012**, *68*, 1460-1465.

[56] W. P. Unsworth, J. D. Cuthbertson, R. J. Taylor, *Org. Lett.* **2013**, *15*, 3306-3309.

[57] M. Kandasamy, B. Ganesan, M. Y. Hung, W. Y. Lin, *Eur. J. Org. Chem.* **2019***,* 20, 3183-3189.

[58] R. E. Whittaker, A. Dermenci, G. Dong, *Synthesis*, **2016**, *48*, 161-183.

[59] M. Schuler, F. Silva, C. Bobbio, A. Tessier, V. Gouverneur, *Angew. Chem. Int. Ed.* **2008**, *47*, 7927-7930.

[60] J. D. Kirkham, S. J. Edeson, S. Stokes, J. P. Harrity, *Org. Lett.* **2012**, *14*, 5354-5357.

[61] C. François-Endelmond, T. Carlin, P. Thuery, O. Loreau, F. Taran, *Org. Lett.* **2009**, *12*, 40-42.

[62] S. G. Huang, H. F. Mao, S. F. Zhou, J. P. Zou, W. Zhang, *Tetrahedron Lett.* **2013**, *54*, 6178-6180.

[63] N. Li, D. Wang, J. Li, W. Shi, C. Li, B. Chen, *Tetrahedron Lett.* **2011**, *52*, 980-982.

[64] O. Seppaenen, M. Muuronen, J. Helaja, *Eur. J. Org. Chem* **2014***, 19,* 4044-4052.

[65] Z. Lian, M. Shi, *Eur. J. Org. Chem*, **2012**, 581.

[66] J. W. Kroeger, J. A. Nieuwland, *J. Am. Chem. Soc.* **1936**, *58*, 1861-1863.

[67] R. B. Davis, D. H. Scheiber, *J. Am. Chem. Soc.* **1956**, *78*, 1675-1678.

[68] O. G. *Yashina*, T. V. *Zarva*, T. D. *Kaigorodova*, L. I. *Vereshchagin*, *J. Org. Chem*. ***1968****, 4, 2104–2107.*

[69] D. R. M. Walton, F. J. Waugh, *Organomet. Chem.* **1972**, *37*, 45**.**

[70] MW. *Logue*, G. L. *Moore, J. Org*. *Chem*. ***1975****, 40,* 131– 132*.*

[71] MW. Logue, K. Teng, *J. Org. Chem.* **1982**, *47*, 2549–2553.

[72] HC. Brown, US. Racherla, SM. Singh, *Tetrahedron Lett.* **1984**, *25*, 2411–2414.

[73] Y. Han, L. Fang, WT. Tao, YZ. Huang, *Tetrahedron Lett*. **1995***, 36*, 1287–1290.

[74] N. Kakusawa, K. Yamaguchi, J. Kurita, T. Tsuchiya, *Tetrahedron Lett.* **2000**, *41*, 4143–4146.

[75] I. Pérez, JP. Sestelo, LA. Sarandeses, *J. Am. Chem. Soc.* **2011**, *123,* 4155–4160.

[76] KY. Lee, MJ. Lee, JN. Kim, *Tetrahedron.* **2005***, 61*, 8705–8710.

[77] Y. Nishihara, D. Saito, E. Inoue, Y. Okada, M. Miyazaki, Y. Inoue, *Tetrahedron Lett.* **2010**, *51*, 306–308.

[78] L. Ge, C. Han, J. Liu, *Journal of Materials Chemistry*, **2012**, *22*, 11843-11850.

[79] S. B. Patel, D. V. Vasava, *ChemistrySelect* **2018**, *3*, 471-480.

[80] D. Liu, Y. Liu, P. Huang, C. Zhu, Z. Kang, J. Shu, M. Chen, X. Zhu, J. Guo, L. Zhuge, X. Bu, P. Feng, T. Wu, *Angew. Chem. Int.l Ed.* **2018,** *57*,

5374-5378.

[81] K. Qi, Y. Li, Y. Xie, S. Y. Liu, K. Zheng, Z. Chen, Z., R. Wang, *Front. chem.*, **2019**, *7,* 1-9..

Entry for the Table of Contents

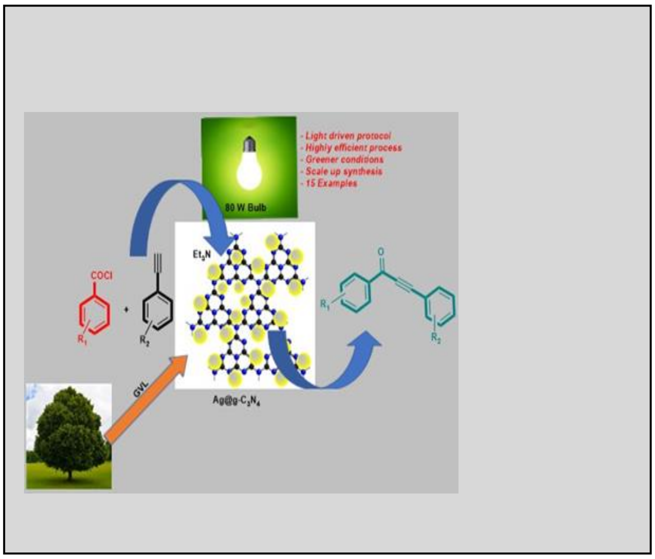

We have developed silver nanocomposite mediated synthesis of various substituted ynones in the presence of visible light. We have utilized the GVL as a greener solvent for the reaction. The use of 80 W tungsten bulb as a visible light source and heterogeneous catalyst makes the process sustainable.